Performance/Design Formulation for a Solid Polymer Based Acid Electrolyte Hydrogen/Air Fuel Cell

S.S. Sandhu[+,a], J.P. Fellner[b]

[a]Department of Chemical and Materials Engineering, University of Dayton
300 College Park, Dayton, OH 45469-0246
[b]Air Force Research Laboratory, Propulsion Directorate, Plans and Analysis Branch, 1950 Fifth Street, Wright-Patterson AFB, OH 45433-7251

Abstract

Mathematical development of preliminary performance/design equations for a hydrogen/air, solid polymer acid electrolyte based fuel cell is presented. The development is based on the principles of transport phenomena, intrinsic electro-chemical kinetics, and classical thermodynamics. The developed formulation is intended to quantitatively describe the mass fraction profiles of the chemical species, hydrogen and oxygen, in the cell anode and cathode diffusion and electrocatalytic reaction layers as a function of the distance in the proton transport direction at an axial distance parallel to the cell anode or cathode channel flow. Given the cell geometry, chemical species and charge transport, and intrinsic electrochemical kinetic parameters, the developed formulation can be employed to compute the species local mass fluxes and predict the cell anode and cathode cell overvoltages for a desired geometric current density. The presented single cell performance predictive formulation has also been linked to the formulation needed to predict the performance of a stack of a number of identical PEMFCs connected in series.

[+]*Corresponding author: e-mail address: Sarwan.Sandhu@notes.udayton.edu*

1. Introduction

Recent PEMFC modeling activity is found in the references.[1-38] Most of the PEMFC models are shown to simulate the overall fuel cell performance reasonably well. A detailed review of these PEMFC models, due to space limitations, will be provided at a later date.

The mathematical formulation, detailed in the next section, is for a hydrogen/air PEMFC utilizing, for example, Nafion, PBO(poly(p-phenylene-2,6 benzobisoxazole))/PBI (poly(benzimidazole)) based phosphoric acid, or sulfonated polyarylene ether or Nafion-Teflon-$Zr(HPO_4)_2$ as an electrolyte. This two-dimensional model, originally developed for a PEMFC fueled by hydrogen gas, can be extended to predict the performance of PEMFC fueled by a gas mixture containing hydrogen, carbon monoxide, small amount of oxygen, carbon dioxide and nitrogen as found in the gas mixture issuing from a reformer dedicated for the production of fuels for fuel cell applications.[39]

2. Mathematical Formulation

Figure 1 shows the schematic of a single proton exchange membrane fuel cell (PEMFC). Operation of such a PEMFC is assumed to be under the isothermal and steady-

state conditions. Hydrogen gas or gas mixture, containing hydrogen, nitrogen, carbon dioxide, etc., from a reformer enters the anode channel and flows in the x-direction. At any x-location, hydrogen diffuses from the anode channel bulk flow to the porous carbon anode diffusion layer (ADL). Then, it diffuses through the ADL to the interface between the ADL and the anode reaction layer (ARL). The porous reaction layer is composed of catalytic platinum particles, in contact with an acid solid polymer electrolyte such as Nafion or PBO/PBI electrolyte, dispersed on the porous carbon granules. Hydrogen diffuses toward the interface between the ARL and solid polymer electrolyte separator layer sandwiched between the anode and cathode reaction layers. In the ARL, hydrogen, while it diffuses, is consumed via the overall electrochemical reaction given by Eq. (1). The generated electrons enter an external electric circuit to pass through an external electrical load. The generated protons migrate internally through the electrolyte separator to the porous cathode reaction layer (CRL) where they cause reduction of oxygen in the presence of electrons that return from the external electric load to the cathode reaction layer.

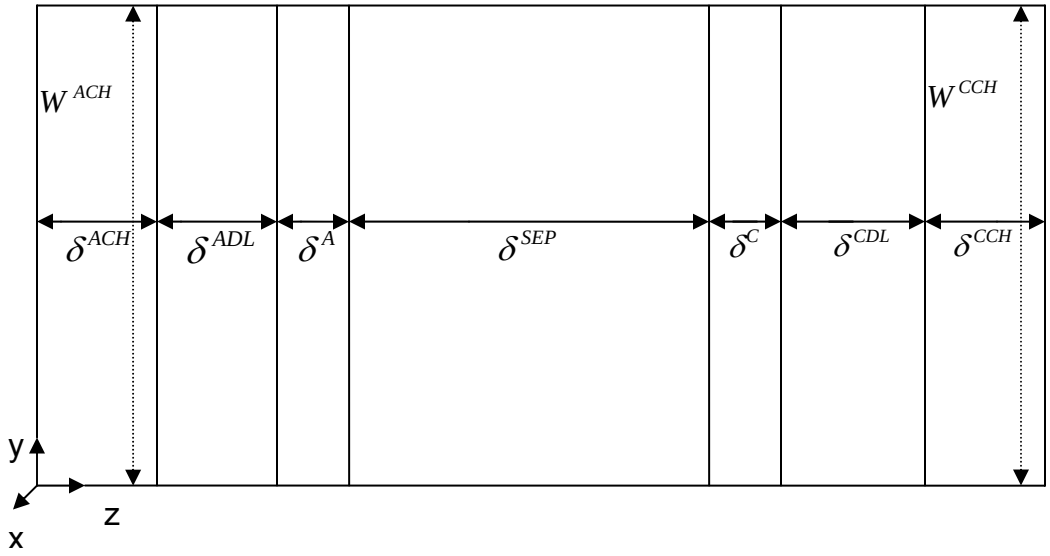

(Note: the x-direction is $\perp$ the y-z plane. Fuel and oxidant gas streams in the anode and cathode channel are parallel to the x-direction. L^{ACH}, L^{CCH}: anode and cathode channel length, respectively, parallel to the x-axis. $\delta^{ACH}, \delta^{ADL}, \delta^{A}, \delta^{SEP}, \delta^{C}, \delta^{CDL}, and\ \delta^{CCH}$ are the dimensions of anode channel, anode diffusion layer, anode reaction layer, solid polymer electrolyte membrane, cathode reaction layer, cathode diffusion layer, and cathode channel, respectively, parallel to the z-axis. W^{ACH} and W^{CCH} are the anode and cathode channel dimensions, respectively, parallel to the y- axis.)

Figure 1. Schematic of a single fuel cell.

Atmospheric air, containing some water vapor, enters the cathode-side flow channel. At any x-location in the flow channel, oxygen diffuses toward the cathode reaction layer along the z-direction, but opposite to an increase in the z-value. Oxygen first diffuses through the

chemical species concentration boundary layer to the porous carbon cathode diffusion layer (CDL). The chemical species concentration boundary layer may or may not prevail at the porous surface of the CDL depending on the oxygen reduction rate in the CRL and the cathode channel flow Reynolds number value. It then diffuses through the CDL to the interface between the CDL and relatively thinner CRL. The porous CRL is composed of catalytic platinum particles, in contact with an acid solid polymer electrolyte, for example, Nafion or PBO/PBI, dispersed on the porous carbon granules. In the CRL, oxygen diffuses toward the interface between the CRL and solid polymer acid electrolyte separator layer, while it is simultaneously consumed via the following overall electrochemical reduction reaction as given by Eq. (2). The electrochemically produced water in the cathode reaction layer diffuses through the cathode reaction and diffusion layers. It, then, diffuses through the species concentration boundary layer prevailing at the porous CDL surface to join the cathode channel bulk flow. It is here noted that the oxygen mass transport is in the direction of decreasing z- while water vapor transport is in the opposite direction. Transport of the gaseous species through the solid polymer electrolyte separator layer is assumed to be negligibly small.

Given below are the main mathematical model equations. One may find the detail behind the formulation development elsewhere.[40]

The half cell reactions at the anode and cathode electrocatalytic reaction layers, respectively, are:

$$H_2 \rightleftarrows 2H^+ + 2e^- \tag{1}$$

$$\frac{1}{2}O_{2(g)} + 2H^+ + 2e^- \rightleftarrows H_2O_{(g)} \tag{2}$$

The overall cell reaction is:

$$H_{2(g)} + \frac{1}{2}O_{2(g)} \rightleftarrows H_2O \tag{3}$$

The reversible cell voltage is given by

$$E_{rev}^{cell} = E^{\circ} + \frac{RT}{2F}\ln\left[\frac{\dfrac{p_{H_2}}{p^{\circ}}\left(\dfrac{p_{O_2}}{p^{\circ}}\right)^{\frac{1}{2}}}{a_{H_2O}}\right] \tag{4}$$

where E° = standard-state reversible cell voltage at the cell temperature corresponding to the unit activities of the chemical species; a_{H_2O} = water activity, $a_{H_2O} = \dfrac{p_{H_2O_{(g)}}}{p_{H_2O}^{sat'd\ vapor}}$, if water is in gas phase, $a_{H_2O_{(l)}}$ = 1, if water is in liquid phase; p_{H_2}, p_{O_2}, $p_{H_2O_{(g)}}$ = partial pressure of hydrogen in the bulk gas flow in the anode-side channel exit, and partial pressures of oxygen and water vapor in the bulk gas flow in the cathode-side channel exit, respectively; p°, $p_{H_2O}^{sat'd\ vapor}$ = standard-state pressure (1 atm or bar), and saturated vapor pressure of water at the cell temperature, T, respectively; F = Faraday's constant = 96487 Coulomb per g-equivalent; R = universal gas constant = 8.314 J mol^{-1}K^{-1}. In the denominator of Eq. (4), the constant 2 corresponds to 2 g-moles of H^+ or e^- per 1 g-mole of H_2 consumed electrochemically.

Total ohmic voltage loss in the electrolyte separator, anode and cathode diffusion and electrocatalytic reaction layers is given by

$$\eta_{\Omega}^{t} = \eta_{\Omega}^{SEP} + \left(\eta_{\Omega}^{ADL} + \eta_{\Omega}^{CDL}\right) + \left(\eta_{\Omega}^{A} + \eta_{\Omega}^{C}\right) \tag{5}$$

The formulation to compute η_{Ω}^{SEP}, η_{Ω}^{ADL}, η_{Ω}^{CDL}, η_{Ω}^{A}, and η_{Ω}^{C}; the ohmic voltage loss in the membrane separator, anode and cathode diffusion, and anode and cathode reaction layer, respectively, is given elsewhere.[40]

2.1 The fuel cell anode-side formulation

The flux of a chemical species α in the z-direction at an x-location through the fluid phase concentration boundary layer prevailing at the porous anode carbon diffusion layer (ADL), in general, is given by

$$\dot{N}_{\alpha,eff,z} = k_{c,\alpha}^{ACH} \varepsilon_{g}^{ADL} (c_{\alpha}^{ACH} - c_{\alpha-\delta^{ACH}}) \tag{6}$$

where α = H_2, N_2, CO_2, H_2O, etc. The mass flux of a chemical species α in the z-direction through the concentration boundary layer is given by

$$\dot{n}_{\alpha,eff,z} = \dot{N}_{\alpha,eff,z} M_{\alpha} = k_{c,\alpha}^{ACH} \varepsilon_{g}^{ADL} M^{ACH} c^{ACH} (\omega_{\alpha}^{ACH} - \omega_{\alpha-\delta^{ACH}}) \tag{6a}$$

where $k_{c,\alpha}^{ACH}$ = mass transfer coefficient for the transport of a chemical species α in the z-direction, [cm s^{-1}], in the anode channel flow. Its value can be determined using the semiempirical equations.[40, 41] c_{α}^{ACH} = bulk concentration of a chemical species α in the anode channel fluid flow, [mol cm^{-3}]; $c_{\alpha-\delta^{ACH}}$ = gas phase concentration of a chemical species α at the surface of the porous ADL facing the anode channel bulk flow, [mol cm^{-3}]; ε_{g}^{ADL} = void fraction of the gas-filled pores in the porous carbon ADL; M_{α} = molecular weight of a species α, [gm mol^{-1}]; M^{ACH} = gas mixture molecular weight in the anode channel; c^{ACH} = gas mixture molar concentration in the anode channel, [mol cm^{-3}]; P^{ACH} = total pressure in the anode channel, [atm or bar]; y_{α}^{ACH} = mole fraction of species α in the anode channel at an x-location; R = universal gas constant = 83.14 cm^3 bar $mol^{-1}K^{-1}$.

Mass flux equation for a chemical species for its transport through the porous carbon anode diffusion layer in mass units, [g $cm^{-2}s^{-1}$], is given as

$$\dot{n}_{\alpha,eff,z} = -\rho D_{\alpha,eff}^{ADL} \frac{d\omega_{\alpha}}{dz} + \omega_{\alpha} \sum_{\beta} \dot{n}_{\beta,eff,z} \tag{7}$$

where α,β= H_2, N_2, CO_2, H_2O, etc., and

$$D_{\alpha,eff}^{ADL} = \frac{D_{\alpha-gas}^{ADL} \varepsilon_{g}^{ADL}}{\tau_{p(g)}^{ADL}} \tag{7a}$$

where $D_{\alpha-gas}^{ADL}$ = mass diffusivity of a chemical species, α, in the gas phase mixture in the ADL pores, [cm^2 s^{-1}]. Correction for the Knudsen diffusion effect on the species transport in the pores should be included if the average pore radius is less than 10 nm or 100 Å. ω_{α} = mass fraction of a chemical species α in the gas mixture; ε_{g}^{ADL} = volume fraction of the gas filled pores in the porous carbon ADL; $\tau_{p(g)}^{ADL}$ = tortuosity factor of the gas filled pores in the ADL.

For the assumption of $\dot{n}_{\alpha,eff,z}$ =0, [β=N_2, CO_2, H_2O], with α = H_2, Eq. (7) reduces to

$$\dot{n}_{H_2,eff,z} = \frac{\rho D^{ADL}_{H_2,eff}}{\left(1-\omega_{H_2}\right)}\left(\frac{-d\omega_\alpha}{dz}\right) \tag{8}$$

Equation (8) is solved for ω_{H_2}, with the boundary condition, at z = δ^{ACH}, $\omega_{H_2} = \omega_{H_2-\delta^{ACH}}$ = mass fraction of hydrogen in the gas mixture at the porous surface of the carbon ADL facing the anode channel flow. The result is

$$\omega_{H_2} = 1-\left(1-\omega_{H_2,\delta^{ACH}}\right)\exp\left[\left(\frac{\dot{n}_{H_2,eff,z}}{\rho D^{ADL}_{H_2,eff}}\right)\left(z-\delta^{ACH}\right)\right] \tag{9}$$

valid for $\delta^{ACH} \le z \le \left(\delta^{ACH}+\delta^{ADL}\right)$. Equation (6a) is used to eliminate $\omega_{H_2,\delta^{ACH}}$ from Eq. (9) to obtain

$$\omega_{H_2} = 1-\left\{1-\omega^{ACH}_{H_2}+\frac{\dot{n}_{H_2,eff,z}}{k^{ACH}_{c,H_2}\varepsilon^{ADL}_g M^{ACH} c^{ACH}}\right\}\exp\left[\left(\frac{\dot{n}_{H_2,eff,z}}{\rho D^{ADL}_{H_2,eff}}\right)\left(z-\delta^{ACH}\right)\right] \tag{10}$$

valid for $\delta^{ACH} \le z \le \left(\delta^{ACH}+\delta^{ADL}\right)$. Equation (10) can be employed to calculate the mass fraction of hydrogen, ω_{H_2}, as a function of distance z in the porous carbon anode diffusion layer provided $n_{H_2,eff,z}$, corresponding to a geometric current density, i_{geom}, and the anode channel bulk gas concentration of H_2, $\omega^{ACH}_{H_2}$, at an x-location are known.

For the assumption of hydrogen transport in the relatively thin anode reaction layer via molecular mass diffusion, the hydrogen mass transport flux in the z-direction in the anode reaction layer is given by

$$\dot{n}^{ARL}_{H_2,eff,z} = \rho D^{ARL}_{H_2,eff}\left(\frac{-d\omega_{H_2}}{dz}\right) \tag{11}$$

A mass balance for hydrogen over a thin spatial element in the anode reaction layer was applied to obtain the following differential equation accounting for the simultaneous transport and consumption of hydrogen via electrochemical reaction.

$$\frac{d\dot{n}^{ARL}_{H_2,eff,z}}{dz} = -\left(\frac{i^A_{o,s}}{2F}\right)a^A M_{H_2}\exp\left[\frac{\alpha^A_a\left|\eta^A\right|F}{RT}\right] \tag{12}$$

On substitution for $\dot{n}^{ARL}_{H_2,eff,z}$ from Eq. (11) into Eq. (12), for the assumption of constant $\left(\rho D^{ARL}_{H_2,eff}\right)$, the following differential equation was obtained.

$$\frac{d^2\omega_{H_2}}{dz^2} = \left(\frac{i^A_{o,s}}{2F}\right)\left(\frac{a^A M_{H_2}}{\rho D^{ARL}_{H_2,eff}}\right)\exp\left(\frac{\alpha^A_a\left|\eta^A\right|F}{RT}\right) \tag{13}$$

$$\frac{i^A_{o,s}}{2F} = k^A_o\exp\left(\frac{-E^A_o}{RT}\right)p_{H_2} \tag{14a}$$

$$= k_o^A \exp\left(\frac{-E_o^A}{RT}\right)\left(\frac{MP}{M_{H_2}}\right)\omega_{H_2} \tag{14b}$$

The differential equation (13) was solved using the boundary conditions: at $z = \delta^{ACH} + \delta^{ADL}$, $\omega_{H_2} = \omega^{+}_{H_2-\delta-ACH-ADL}$, the hydrogen mass fraction on positive side of the interface between the anode diffusion and reaction layers; at $z = \delta^{ACH} + \delta^{ADL} + \delta^{ARL}$, $\left(\frac{d\omega_{H_2}}{dz}\right)^{-} = 0$ (i.e. spatial gradient of the hydrogen mass fraction on the negative side of the interface between the anode reaction layer and the polymer electrolyte separator layer is zero.) The resulting solution to compute ω_{H_2} as a function of the distance z is given as

$$\omega_{H_2} = \omega^{+}_{H_2-\delta-ACH-DL}\left[\frac{\cosh\left(\sqrt{F_1^A}\, z\right)}{\cosh\left(\sqrt{F_1^A}\, \delta^{ACH-DL}\right)}\right]\left[\frac{1-\tanh\left(\sqrt{F_1^A}\, z\right)\tanh\left(\sqrt{F_1^A}\, \delta^{ACH-DL-RL}\right)}{1-\tanh\left(\sqrt{F_1^A}\, \delta^{ACH-DL}\right)\tanh\left(\sqrt{F_1^A}\, \delta^{ACH-DL-RL}\right)}\right] \tag{15}$$

where,

$$F_1^A = \left[\frac{MPa^A}{\rho D^{ARL}_{H_2,eff}}\right]\left[k_o^A \exp\left(-\left(\frac{E_o^A - \alpha_a^A\left|\eta^A\right|F}{RT}\right)\right)\right], \qquad [cm^{-2}] \tag{15a}$$

$$k_o^A = \left(\frac{i^A_{o,s,T_o,p_{H_2,o}}}{2Fp_{H_2,o}}\right)\exp\left(\frac{E_o^A}{RT_o}\right), \quad [mol\ s^{-1}cm^{-2}atm^{-1}] \tag{15b}$$

$$\delta^{ACH-DL} = \delta^{ACH} + \delta^{ADL} \tag{15c}$$

$$\delta^{ACH-DL-RL} = \delta^{ACH} + \delta^{ADL} + \delta^{ARL} \tag{15d}$$

Equation (15) is valid for $\delta^{ACH-DL} < z \le \delta^{ACH-DL-RL}$. The solution given in Eq. (15) was obtained using the assumption that variation in $\left|\eta^A\right|$ with respect to z in a thin reaction layer is negligibly small. If it is assumed that hydrogen is present in the gas phase across the interface between the anode diffusion and reaction layers, then it is reasonable to assume

$$\omega^{-}_{H_2-\delta-ACH-DL} = \omega^{+}_{H_2-\delta-ACH-DL} \tag{16}$$

Using Eq. (10), the following equation was obtained:

$$\omega^{+}_{H_2-\delta-ACH-DL} = \omega^{-}_{H_2-\delta-ACH-DL} = 1-\left\{1-\omega^{ACH}_{H_2} + \frac{\dot{n}_{H_2,eff,z}}{k^{ACH}_{c,H_2}\varepsilon_g^{ADL}M^{ACH}c^{ACH}}\right\}\exp\left(\frac{\dot{n}_{H_2,eff,z}}{\frac{\rho D^{ADL}_{H_2,eff}}{\delta^{ADL}}}\right) \tag{17}$$

On substitution for $\omega^{+}_{H_2-\delta-ACH-DL}$ from Eq. (17) into Eq. (15), the following equations was obtained to predict ω_{H_2} as a function of the distance z in the anode reaction layer.

$$\omega_{H_2} = \alpha\left[\cosh\left(\sqrt{F_1^A}\, z\right) - \zeta\sinh\left(\sqrt{F_1^A}\, z\right)\right] \tag{18}$$

which is valid for $\delta^{ACH-DL} < z \le \delta^{ACH-DL-RL}$ and where

$$\zeta = \tanh\left(\sqrt{F_1^A}\, \delta^{ACH-DL-RL}\right) \tag{18a}$$

and

$$\alpha = \frac{1-\left\{\left(1-\omega_{H_2}^{ACH}\right)+\dfrac{\dot{n}_{H_2,eff,z}}{k_{c,H_2}\varepsilon_g^{ADL}M^{ACH}c^{ACH}}\right\}\exp\left(\dfrac{\dot{n}_{H_2,eff,z}}{\rho D_{H_2,eff}^{ADL}/\delta^{ADL}}\right)}{\cosh\left(\sqrt{F_1^A}\,\delta^{ACH-DL}\right)\left[1-\tanh\left(\sqrt{F_1^A}\,\delta^{ACH-DL}\right)\right]\left[\tanh\left(\sqrt{F_1^A}\,\delta^{ACH-DL-RL}\right)\right]} \tag{18b}$$

One notes that the prediction of ω_{H_2} as a function of z at an x-plane requires the data on $\dot{n}_{H_2,eff,z}$ corresponding to a geometric current density, transport and electrode electrochemical kinetic parameters, and dimensions of the anode flow channel and diffusion and reaction layers parallel to the z direction.

Equation (18) was used to obtain $\left(\dfrac{-d\omega_{H_2}}{dz}\bigg|_{z=\delta^{ACH-DL}}\right)$ and the result substituted into Eq. (11) to obtain

$$\dot{n}_{H_2,eff,z}^{ARL}\Big|_{z=\delta^{ACH-DL}} = \rho D_{H_2,eff}^{ARL}\alpha\sqrt{F_1^A}\left[\zeta\cosh\left(\sqrt{F_1^A}\,\delta^{ACH-DL}\right)-\sinh\left(\sqrt{F_1^A}\,\delta^{ACH-DL}\right)\right] \tag{19}$$

If at an x-plane, the required geometric current density is i_{geom}, the hydrogen mass flux that must enter the anode reaction layer at $z=\delta^{ACH-DL}=\delta^{ACH}+\delta^{ADL}$ is

$$\dot{n}_{H_2,eff,z}^{ARL}\Big|_{z=\delta^{ACH-DL}} = \left(\frac{i_{geom}}{2F}\right)M_{H_2} \tag{20}$$

On equating the right-hand sides of Eqs. (19) and (20), one obtains the following equation:

$$f_1 = \alpha\sqrt{F_1^A}\left[\zeta\cosh\left(\sqrt{F_1^A}\,\delta^{ACH-DL}\right)-\sinh\left(\sqrt{F_1^A}\,\delta^{ACH-DL}\right)\right] = \left(\frac{i_{geom}}{2F}\right)\left(\frac{M_{H_2}}{\rho D_{H_2,eff}^{ARL}}\right) \tag{21}$$

where $\delta^{ACH-DL}=\delta^{ACH}+\delta^{ADL}$. One should solve Eq. (21) for $\sqrt{F_1^A}$ for a given value of i_{geom} using a method: trial and error, Newton's or graphical method; or any commercial computer software. One can then determine the anode reaction overvoltage $\left|\eta^A\right|$ from Eq. (15a) corresponding to the geometric current density, i_{geom}.

2.2 The fuel cell cathode-side formulation

The flux of O_2 in the z-direction through the gas phase concentration boundary layer prevailing at the porous surface of the carbon cathode diffusion layer (CDL) facing the cathode channel flow is given by

$$\left(-\dot{N}_{O_2,eff,z}\right) = k_{C,O_2}^{CCH}\varepsilon_g^{CDL}\left(c_{O_2}^{CCH}-c_{O_2,z_{fs}^{CDL}}\right) \tag{22}$$

The mass flux of oxygen in the z-direction through the gas phase concentration boundary layer is given by

$$\left(-\dot{n}_{O_2,eff,z}\right) = \left(-\dot{N}_{O_2,eff,z}\right)M_{O_2} = k_{C,O_2}^{CCH}\varepsilon_g^{CDL}M^{CCH}c^{CCH}\left(\omega_{O_2}^{CCH}-\omega_{O_2,z_{fs}^{CDL}}\right) \tag{23}$$

where k_{C,O_2}^{CCH} = mass transfer coefficient for the transport of a chemical species α in the z-direction, [cm s^{-1}], in the cathode channel flow. Its value can be determined using semiempirical equations.[40, 41] c_{α}^{CCH} = bulk concentration of a chemical species α in the cathode channel flow, [mol cm^{-3}], (α = O_2, H_2O, N_2); $c_{\alpha,z_{fs}^{CDL}}$ = gas phase concentration of chemical species α at the porous surface of the carbon diffusion layer facing the cathode bulk channel flow and located at the farside of the CDL, $z_{fs}^{CDL} = \delta^{ACH} + \delta^{ADL} + \delta^{A} + \delta^{SEP} + \delta^{C} + \delta^{CDL}$, [mol cm^{-3}]; ε_g^{CDL} = void fraction of the gas-filled pores in the porous carbon CDL; M^{CCH} = gas mixture molecular weight in the cathode channel, [g mol^{-1}]; P^{CCH} = total pressure in the cathode channel, [bar or atm]; y_{α}^{CCH} = mole fraction of a chemical species α in the cathode channel at an x-location; ω_{α}^{CCH} = weight fraction of a species α. The molar flux of $H_2O_{(v)}$ in the z-direction through the gas phase concentration boundary layer prevailing at the porous surface of the CDL is given by

$$\dot{N}_{H_2O,eff,z} = k_C^{CCH}\varepsilon_g^{CDL}\left(c_{H_2O,z_{fs}^{CDL}} - c_{H_2O}^{CCH}\right) \tag{24}$$

The mass flux of $H_2O_{(v)}$ in the z-direction through the gas phase concentration boundary layer is given by

$$\dot{n}_{H_2O,eff,z} = \dot{N}_{H_2O,eff,z}M_{H_2O} = k_{C,H_2O}^{CCH}\varepsilon_g^{CDL}M^{CCH}c^{CCH}\left(\omega_{H_2O,z_{fs}^{CDL}} - \omega_{H_2O}^{CCH}\right) \tag{25}$$

From Eqs. (23) and (25), one obtains

$$\omega_{O_2,z_{fs}^{CDL}} = \omega_{O_2}^{CCH} - \frac{\left(-\dot{n}_{O_2,eff,z}\right)}{k_{C,O_2}^{CCH}\varepsilon_g^{CDL}M^{CCH}c^{CCH}} \tag{26}$$

$$\omega_{H_2O,z_{fs}^{CDL}} = \omega_{H_2O}^{CCH} + \frac{\dot{n}_{H_2O,eff,z}}{k_{C,H_2O}^{CCH}\varepsilon_g^{CDL}M^{CCH}c^{CCH}} \tag{27}$$

The nitrogen molar flux along the z-direction is assumed zero. That is,

$$\dot{N}_{N_2,eff,z} = 0.0 \tag{28}$$

Also,

$$\dot{n}_{N_2,eff,z} = \dot{N}_{N_2,eff,z}M_{N_2} = 0 \tag{28a}$$

The general mass flux equation, which describes the mass transport of a chemical species α in the CDL by the mass diffusion and convection processes, is given as

$$\dot{n}_{\alpha,eff,z} = \rho D_{\alpha,eff}^{CDL}\left(\frac{-d\omega_{\alpha}}{dz}\right) + \omega_{\alpha}\sum_{\beta}\dot{n}_{\beta,eff,z} \qquad (\alpha, \beta = O_2, H_2O, N_2) \tag{29}$$

Under the steady-state condition at any x,

$$\dot{n}_{O_2,eff,z}\left(\text{at any z within the CDL}\right)=\dot{n}_{O_2,eff,z}\Big|_{z=z_{fs}^{CRL}}$$

$$=\begin{pmatrix}\text{mass flux of } O_2 \text{ reaching the interface between the}\\ \text{cathode diffusion layer (CDL) and reaction layer (CRL)}\end{pmatrix}$$

$$=\begin{pmatrix}\text{consumption rate of } O_2 \text{ in the CRL corresponding to unit}\\ \text{geometric area } \perp z \text{ via the reaction: } 4H^+ + 4e^- + O_2 \rightarrow 2H_2O\end{pmatrix} \tag{30}$$

$$=-\frac{i_{geom}}{4F}M_{O_2}$$

The water mass flux in the z-direction within the CDL at any x- is given as

$$\dot{n}_{H_2O,eff,z}=\begin{pmatrix}\text{water production rate corresponding to the unit geometric}\\ \text{area } \perp \text{ z- via the electrochemical reaction rate}\end{pmatrix}+$$

$$\begin{pmatrix}\text{net water transport rate per unit geometric}\\ \text{area } \perp \text{ z- from the ARL to CRL}\end{pmatrix} \tag{31}$$

$$=\frac{i_{geom}M_{H_2O}}{2F}+\frac{\zeta_{H_2O}i_{geom}M_{H_2O}}{F}=\left(1+2\zeta_{H_2O}\right)\frac{i_{geom}M_{H_2O}}{2F}$$

where ζ_{H_2O} = g-moles of water transported to the CRL per g-mole of H^+ ions migrating from the ARL to CRL, i_{geom} = geometric current density along the z-direction, [A cm^{-2}]. Using the expressions in Eqs. (30), (31), with $\dot{n}_{N_2,eff,z}=0$,

$$\sum_{\beta}\dot{n}_{\beta,eff,z}=\dot{n}_{O_2,eff,z}+\dot{n}_{H_2O,eff,z}+\dot{n}_{N_2,eff,z} \tag{32a}$$

$$=\left(\frac{i_{geom}M_{H_2}}{2F}\right)\left(1+18\zeta_{H_2O}\right) \tag{32b}$$

Combining the information in Eqs. (29) and (32b) to obtain

$$\dot{n}_{\alpha,eff,z}=\rho D_{\alpha,eff}^{CDL}\left(\frac{-d\omega_\alpha}{dz}\right)+\omega_\alpha\left(\frac{i_{geom}M_{H_2}}{2F}\right)\left(1+18\zeta_{H_2O}\right) \tag{33}$$

$$\left(\alpha=O_2,\, H_2O_{(v)},\, N_2\right)$$

where

$$D_{\alpha,eff}^{CDL}=\frac{D_{\alpha,gas}^{CDL}\varepsilon_g^{CDL}}{\tau_{p(g)}^{CDL}} \tag{33a}$$

Equation (33) is transformed to

$$\frac{d\omega_\alpha}{dz}+\left[\frac{-\left(1+18\zeta_{H_2O}\right)\left(\frac{i_{geom}M_{H_2}}{2F}\right)}{\rho D_{\alpha,eff}^{CDL}}\right]\omega_\alpha=\frac{-\dot{n}_{\alpha,eff,z}}{\rho D_{\alpha,eff}^{CDL}} \tag{34}$$

The analytical solution to the differential Eq. (34), with the boundary condition at $z=z_{fs}^{CDL}$ (far-side of CDL with respect to $z=0$), $\omega_\alpha=\omega_{\alpha,fs}^{CDL}$, is given below.

$$\omega_{\alpha} = \omega_{\alpha,fs}^{CDL} \exp\left[\frac{\left(1+18\zeta_{H_2O}\right)\left(\frac{i_{geom}M_{H_2}}{2F}\right)}{\rho D_{\alpha,eff}^{CDL}}\left(z - z_{fs}^{CDL}\right)\right] +$$

$$\frac{\dot{n}_{\alpha,eff,z}}{\left(1+18\zeta_{H_2O}\right)\left(\frac{i_{geom}M_{H_2}}{2F}\right)}\left[1-\exp\left\{\frac{\left(1+18\zeta_{H_2O}\right)\left(\frac{i_{geom}M_{H_2}}{2F}\right)}{\rho D_{\alpha,eff}^{CDL}}\left(z - z_{fs}^{CDL}\right)\right\}\right] \quad (35)$$

valid for a chemical species α in the z-range, $z_{ns}^{CDL} \le z \le z_{fs}^{CDL}; \alpha = O_2, H_2O_{(v)}, N_2$.

z_{ns}^{CDL} (near-side of the cathode diffusion layer with respect to z=0) = $\delta^{ACH} + \delta^{ADL} + \delta^{A} + \delta^{SEP} + \delta^{C}$; z_{fs}^{CDL} = $\delta^{ACH} + \delta^{ADL} + \delta^{A} + \delta^{SEP} + \delta^{C} + \delta^{CDL}$. Equation (35) is applied to the chemical species, N_2, O_2 and $H_2O_{(v)}$, respectively, in conjunction with Eqs. (28a), (30), and (31), to obtain

$$\omega_{N_2} = \omega_{N_2,fs}^{CDL} \exp\left[\frac{\left(1+18\zeta_{H_2O}\right)\left(\frac{i_{geom}M_{H_2}}{2F}\right)}{\rho D_{N_2,eff}^{CDL}}\left(z - z_{fs}^{CDL}\right)\right] \quad (36)$$

$$\omega_{O_2} = \omega_{O_2,fs}^{CDL} \exp\left[\frac{\left(1+18\zeta_{H_2O}\right)\left(\frac{i_{geom}M_{H_2}}{2F}\right)}{\rho D_{O_2,eff}^{CDL}}\left(z - z_{fs}^{CDL}\right)\right] - \left(\frac{8}{1+18\zeta_{H_2O}}\right)*$$

$$\left[1-\exp\left\{\frac{\left(1+18\zeta_{H_2O}\right)\left(\frac{i_{geom}M_{H_2}}{2F}\right)}{\rho D_{O_2,eff}^{CDL}}\left(z - z_{fs}^{CDL}\right)\right\}\right] \quad (37)$$

$$\omega_{H_2O} = \omega_{H_2O,fs}^{CDL} \exp\left[\frac{\left(1+18\zeta_{H_2O}\right)\left(\frac{i_{geom}M_{H_2}}{2F}\right)}{\rho D_{H_2O,eff}^{CDL}}\left(z - z_{fs}^{CDL}\right)\right] + 9\left(\frac{1+2\zeta_{H_2O}}{1+18\zeta_{H_2O}}\right)*$$

$$\left[1-\exp\left\{\frac{\left(1+18\zeta_{H_2O}\right)\left(\frac{i_{geom}M_{H_2}}{2F}\right)}{\rho D_{H_2O,eff}^{CDL}}\left(z - z_{fs}^{CDL}\right)\right\}\right] \quad (38)$$

The mathematical expressions for $\left(-\dot{n}_{O_2,eff,z}\right)$ and $\dot{n}_{H_2O,eff,z}$ are substituted into Eqs. (26) and (27) to obtain the expressions for $\omega_{O_2,z_{fs}^{CDL}}$ and $\omega_{H_2O,z_{fs}^{CDL}}$. The resulting expressions for $\omega_{O_2,z_{fs}^{CDL}}$, $\omega_{H_2O,z_{fs}^{CDL}}$, and $\omega_{N_2,z_{fs}^{CDL}}=\omega_{N_2}^{CCH}$ are substituted, respectively, into Eqs. (37), (38), and (36) to obtain the following expressions:

$$\omega_{O_2}=\left[\omega_{O_2}^{CCH}-\frac{\left(\frac{i_{geom}M_{O_2}}{4F}\right)}{k_{C,O_2}^{CCH}\varepsilon_g^{CDL}M^{CCH}c^{CCH}}\right]\exp\left[\frac{\left(1+18\zeta_{H_2O}\right)\left(\frac{i_{geom}M_{H_2}}{2F}\right)}{\rho D_{O_2,eff}^{CDL}}\left(z-z_{fs}^{CDL}\right)\right]- \frac{8}{1+18\zeta_{H_2O}}\left[1-\exp\left\{\frac{\left(1+18\zeta_{H_2O}\right)\left(\frac{i_{geom}M_{H_2}}{2F}\right)}{\rho D_{O_2,eff}^{CDL}}\left(z-z_{fs}^{CDL}\right)\right\}\right] \tag{39}$$

$$\omega_{H_2O}=\left[\omega_{H_2O}^{CCH}+\frac{\left(1+2\zeta_{H_2O}\right)\left(\frac{i_{geom}M_{H_2O}}{2F}\right)}{k_{C,H_2O}^{CCH}\varepsilon_g^{CDL}M^{CCH}c^{CCH}}\right]\exp\left[\frac{\left(1+18\zeta_{H_2O}\right)\left(\frac{i_{geom}M_{H_2}}{2F}\right)}{\rho D_{H_2O,eff}^{CDL}}\left(z-z_{fs}^{CDL}\right)\right]+ 9\left(\frac{1+2\zeta_{H_2O}}{1+18\zeta_{H_2O}}\right)\left[1-\exp\left\{\frac{\left(1+18\zeta_{H_2O}\right)\left(\frac{i_{geom}M_{H_2}}{2F}\right)}{\rho D_{H_2O,eff}^{CDL}}\left(z-z_{fs}^{CDL}\right)\right\}\right] \tag{40}$$

$$\omega_{N_2}=\omega_{N_2}^{CCH}\exp\left[\frac{\left(1+18\zeta_{H_2O}\right)\left(\frac{i_{geom}M_{H_2}}{2F}\right)}{\rho D_{N_2,eff}^{CDL}}\left(z-z_{fs}^{CDL}\right)\right] \tag{41}$$

The equations (39), (40), and (41) can be used to predict the mass fraction profiles of oxygen, water vapor and nitrogen in the gas-filled pores of the cathode diffusion layer (CDL) for $z_{ns}^{CDL}\le z\le z_{fs}^{CDL}$. The mass fractions of the chemical species oxygen, water, and nitrogen at the interface between the CRL and CDL, but on the CDL-side, are obtained by setting $z=z_{ns}^{CDL}$, with $\left(z_{ns}^{CDL}-z_{fs}^{CDL}\right)=-\delta^{CDL}$.

$$\omega^{+}_{O_2,z^{CDL}_{ns}} = \left[\omega^{CCH}_{O_2} - \frac{\left(\frac{i_{geom}M_{O_2}}{4F}\right)}{k^{CCH}_{C,O_2}\varepsilon^{CDL}_{g}M^{CCH}c^{CCH}}\right]\exp\left[\frac{-\left(1+18\zeta_{H_2O}\right)\left(\frac{i_{geom}M_{H_2}}{2F}\right)}{\rho D^{CDL}_{O_2,eff}}\delta^{CDL}\right] - \frac{8}{1+18\zeta_{H_2O}}\left[1-\exp\left\{\frac{-\left(1+18\zeta_{H_2O}\right)\left(\frac{i_{geom}M_{H_2}}{2F}\right)}{\rho D^{CDL}_{O_2,eff}}\delta^{CDL}\right\}\right] \quad (42)$$

$$\omega^{+}_{H_2O,z^{CDL}_{ns}} = \left[\omega^{CCH}_{H_2O} + \frac{\left(1+2\zeta_{H_2O}\right)\left(\frac{i_{geom}M_{H_2O}}{2F}\right)}{k^{CCH}_{C,H_2O}\varepsilon^{CDL}_{g}M^{CCH}c^{CCH}}\right]\exp\left[\frac{-\left(1+18\zeta_{H_2O}\right)\left(\frac{i_{geom}M_{H_2}}{2F}\right)}{\rho D^{CDL}_{H_2O,eff}}\delta^{CDL}\right] + 9\left(\frac{1+2\zeta_{H_2O}}{1+18\zeta_{H_2O}}\right)\left[1-\exp\left\{\frac{-\left(1+18\zeta_{H_2O}\right)\left(\frac{i_{geom}M_{H_2}}{2F}\right)}{\rho D^{CDL}_{H_2O,eff}}\delta^{CDL}\right\}\right] \quad (43)$$

$$\omega^{+}_{N_2,z^{CDL}_{ns}} = \omega^{CCH}_{N_2}\exp\left[\frac{-\left(1+18\zeta_{H_2O}\right)\left(\frac{i_{geom}M_{H_2}}{2F}\right)\delta^{CDL}}{\rho D^{CDL}_{N_2,eff}}\right] \quad (44)$$

In the cathode reaction layer, oxygen is transported as well as reduced via the electrochemical reaction, $O_{2(g)} + 4\left(H^{+} + e^{-}\right) \rightarrow 2H_2O_{(g)}$, at the catalyst platinum-electrolyte active sites-(s) to produce water. If the first electron transfer step, $O_2 - s + H^{+} + e^{-} \rightarrow HO_2 - s$, is assumed the rate-limiting step in the kinetic mechanism of the overall oxygen reduction process, the oxygen reduction rate per unit active surface area of the electrocatalyst is given by

$$\left(-r_{O_2}\right) = \left(\frac{i^{C}_{o,s}}{4F}\right)\exp\left(\frac{\alpha^{C}_{c}\left|\eta^{C}\right|F}{RT}\right), \quad \left[\text{moles of } O_2 \text{ consumed } s^{-1}cm^{-2}\right] \quad (45)$$

where the cathodic exchange current density, $i^{C}_{o,s}$, is given by

$$i^{C}_{o,s} = i^{C}_{o,s,T_o,p_{O_2},o}\exp\left[\frac{E^{C}_{o}}{R}\left(\frac{1}{T_o}-\frac{1}{T}\right)\right]\left(\frac{p_{O_2}}{p_{O_2},o}\right)^{n} \quad (46)$$

For the first electron transfer step as the kinetic rate-limiting elementary step, the reaction order, n=1.[42] In Eq. (46), $i^{C}_{o,s,T_o,p_{O_2},o}$ = exchange current density for the cathode electrocatalyst at some known reference temperature, T_o, and oxygen partial pressure, p_{O_2},o; E^{C}_{o} =reaction

activation energy for the oxygen reduction reaction, [J mol^{-1}]. T, p_{O_2} = temperature[K] and partial pressure of O_2 [bar or atm] at the electrocatalyst surface, respectively. In Eq. (45), α_c^C = charge transfer coefficient for the cathodic utilization of electrons at the cathode reaction layer electrocatalyst active sites. $\left|\eta^C\right|$ = magnitude of the overvoltage or electrochemical kinetic activation voltage loss for the dominant occurrence of the cathodic (i.e. electron utilization process at the cell cathode, [V].

Oxygen diffuses toward the solid polymer electrolyte separator layer along z-coordinate in the direction of decreasing z while being reduced by the electrochemical reaction at the electrocatalyst interface effective active sites. Based on the coupled oxygen transport and electrochemical reduction processes, a differential model describing the oxygen mass fraction variation with distance z, obtained by the application of steady-state oxygen mass balance over a spatial element, is given by

$$\rho D_{O_2,eff}^{CRL} \frac{d^2\omega_{O_2}}{dz^2} = \left(-R_{O_2,mass}^C\right) \tag{47}$$

In the derivation of Eq. (47), the product of gas mixture density and effective oxygen mass diffusivity, i.e. $\rho D_{O_2,eff}^{CDL}$, was assumed invariant with respect to z in the thin cathode reaction layer (CRL). The gas mixture density ρ may be taken equal to that in the cathode channel gas mixture at an x-location as a first approximation.

For the first-order reaction with respect to oxygen (n=1), with $p_{O_2} = y_{O_2} P^{CCH} = \frac{M\omega_{O_2}}{M_{O_2}} P^{CCH}$, using the expression for $i_{o,s}$ in Eq. (46); the oxygen consumption rate per unit CRL volume is given by

$$\left(-R_{O_2,mass}^C\right) = \left(\frac{i_{o,s,T_o,p_{O_2,o}} Ma^C}{4F}\right)\left(\frac{P^{CCH}}{p_{O_2,o}}\right)\exp\left\{\frac{E_o^C}{R}\left(\frac{1}{T_o}-\frac{1}{T}\right)+\frac{\alpha_c^C\left|\eta^C\right|F}{RT}\right\}\omega_{O_2} \quad \left[\frac{\text{g O}_2\ consumed}{s-cm^3\ of\ CRL}\right] \tag{48}$$

Substitution for $\left(-R_{O_2,mass}^C\right)$ from (48) into (47) leads to

$$\frac{d^2\omega_{O_2}}{dz^2} = F_1^C \omega_{O_2} \tag{49}$$

where

$$F_1^C = \left(\frac{i_{o,s,T_o,p_{O_2}}^C a^C M^{CCH}}{4F\left(\rho^{CCH} D_{O_2,eff}^{CRL}\right)}\right)\left(\frac{P^{CCH}}{p_{O_2,o}}\right)\exp\left\{\frac{E_o^C}{R}\left(\frac{1}{T_o}-\frac{1}{T}\right)+\frac{\alpha_c^C\left|\eta^C\right|F}{RT}\right\}, \quad \left[\frac{1}{cm^2}\right] \tag{49a}$$

For the isothermal condition, with the assumption of constant $\left|\eta^C\right|$ in the relatively thin cathode reaction layer, Eq. (49) was solved using the following boundary conditions:

$$\text{At } z = z_{ns}^{CRL} = \delta^{ACH} + \delta^{ADL} + \delta^{A} + \delta^{SEP}, \qquad \left(\frac{d\omega_{O_2}}{dz}\right)^{+} = 0 \tag{50a}$$

(i.e. the spatial gradient of the oxygen mass fraction on the positive side of the interface between the polymer electrolyte separator layer and cathode reaction layer is zero.)

$$\text{At } z = z_{fs}^{CRL} = \delta^{ACH} + \delta^{ADL} + \delta^{A} + \delta^{SEP} + \delta^{C}, \qquad \omega_{O_2} = \omega_{O_2,fs}^{CRL-} \tag{50b}$$

where $\omega_{O_2,fs}^{CRL-}$ = mass fraction of oxygen on the negative side of the interface between the CRL and CDL. The solution to the differential Eq. (49) is given as

$$\omega_{O_2} = \alpha_1 \left[\cosh\left(\sqrt{F_1^C}\ z\right) - \zeta_1 \sinh\left(\sqrt{F_1^C}\ z\right) \right] \tag{51}$$

(valid for $z_{ns}^{CRL} = \left(\delta^{ACH} + \delta^{ADL} + \delta^{A} + \delta^{SEP}\right) \le z \le z_{fs}^{CRL} = \left(\delta^{ACH} + \delta^{ADL} + \delta^{A} + \delta^{SEP} + \delta^{C}\right)$)

where

$$\alpha_1 = \frac{\omega_{O_2,fs}^{CRL,-}}{\cosh\left(\sqrt{F_1^C}\ z_{fs}^{CRL}\right)\left[1 - \tanh\left(\sqrt{F_1^C}\ z_{ns}^{CRL}\right)\tanh\left(\sqrt{F_1^C}\ z_{fs}^{CRL}\right)\right]} \tag{51a}$$

It is reasonable to assume

$$\omega_{O_2,fs}^{CRL,-} = \omega_{O_2,z_{ns}^{CDL}}^{CRL,+} \tag{52}$$

Using the information provided for $\omega_{O_2,z_{ns}^{CDL}}^{+}$ in Eq. (42) in conjunction with Eq. (52), Eq. (51a) becomes

$$\alpha_1 = \frac{\left[\omega_{O_2}^{CCH} - \dfrac{\dfrac{i_{geom} M_{O_2}}{4F}}{k_{C,O_2}^{CCH} \varepsilon_g^{CDL} M^{CCH} c^{CCH}}\right] \exp\left[\dfrac{-\left(1+18\zeta_{H_2O}\right)\left(\dfrac{i_{geom} M_{H_2}}{2F}\right)\delta^{CDL}}{\rho D_{O_2,eff}^{CDL}}\right]}{\cosh\left(\sqrt{F_1^C}\ z_{fs}^{CRL}\right)\left[1 - \tanh\left(\sqrt{F_1^C}\ z_{ns}^{CRL}\right)\tanh\left(\sqrt{F_1^C}\ z_{fs}^{CRL}\right)\right]} -$$

$$\frac{\dfrac{8}{1+18\zeta_{H_2O}}\left[1 - \exp\left\{\dfrac{-\left(1+18\zeta_{H_2O}\right)\left(\dfrac{i_{geom} M_{H_2}}{2F}\right)\delta^{CDL}}{\rho D_{O_2,eff}^{CDL}}\right\}\right]}{\cosh\left(\sqrt{F_1^C}\ z_{fs}^{CRL}\right)\left[1 - \tanh\left(\sqrt{F_1^C}\ z_{ns}^{CRL}\right)\tanh\left(\sqrt{F_1^C}\ z_{fs}^{CRL}\right)\right]} \tag{53}$$

$$\zeta_1 = \tanh\left(\sqrt{F_1^C}\ z_{ns}^{CRL}\right) \tag{54}$$

Equation (51) can be employed to predict the oxygen mass fraction profile in the cathode reaction layer as a function of distance z. At an x-plane, the oxygen mass flux along the z-direction is given by

$$\left(-\dot{n}_{O_2,eff,z}\right) = \rho^{CCH} D_{O_2,eff}^{CRL} \left(\left.\frac{d\omega_{O_2}}{dz}\right|_{z=z_{fs}^{CRL}} \right) \tag{55a}$$

$$= \frac{i_{geom} M_{O_2}}{4F} \tag{55b}$$

Using the information provided for ω_{O_2} in Eq. (51), in conjunction with Eqs. (55a) and (55b), the following result is obtained.

$$\frac{i_{geom} M_{O_2}}{4F} = \rho^{CCH} D_{O_2,eff}^{CRL} \left(\alpha_1 \sqrt{F_1^C}\right)\left[\sinh\left(\sqrt{F_1^C}\ z_{fs}^{CRL}\right) - \zeta_1 \cosh\left(\sqrt{F_1^C}\ z_{fs}^{CRL}\right)\right] \tag{56}$$

Equation (56) can be re-arranged as

$$\left(\frac{i_{geom} M_{O_2}}{4F \rho^{CCH} D_{O_2,eff}^{CRL}}\right) = \left(\alpha_1 \sqrt{F_1^C}\right)\left[\sinh\left(\sqrt{F_1^C}\ z_{fs}^{CRL}\right) - \zeta_1 \cosh\left(\sqrt{F_1^C}\ z_{fs}^{CRL}\right)\right] \tag{57}$$

For the steady operation of a fuel cell, Eq. (57) can be solved for F_1^C by a trial-error or graphical procedure for a fixed value of i_{geom} at an x-plane. Then, using the defining Eq. (49a) for F_1^C, one can obtain the cathodic electrochemical reaction activation voltage loss, $\left|\eta^C\right|$, for a fixed i_{geom} value at an x-plane. Also, one can find the average cathodic activation voltage loss, $\left|\eta^C\right|_{ave}$ using the cell average current density, $i_{geom,avg} = \left(\frac{\text{cell total current}}{\text{total geometric area of an electrode}}\right)$. It is noted here that the cell anode geometric area (i.e. $L^{ACH} W^{ACH}$) = the cell cathode geometric area (i.e. $L^{CCH} W^{CCH}$). This rigorous mathematical formulation shows how one can obtain the activation voltage loss at the cathode reaction layer by taking into account the effect of mass transport of oxygen through the various layers of the cell on the CRL side.

The mathematical expressions to compute the chemical species molar flow rates at any x-location in the anode and cathode channels have been provided.[40]

3. Application of the developed formulation

The formulation provided in Section 2 may be employed to calculate an average cell voltage at a given or desired average current density for a hydrogen/air PEMFC, using an acid electrolyte medium, for example, Nafion-Teflon-Zr$(HPO_4)_2$ composite[42], PBO/PBI doped with phosphoric acid, or sulfonated poly(arylene ether sulfone)[43]. Example operational conditions are; an elevated temperature, for example, 110 $^{\circ}$C, 1 atm. total pressure, with the water vapor partial pressure slightly less than saturated vapor pressure in the anode-side hydrogen fuel stream and 50% or even lower relative humidity in the cathode-side oxidant air stream to maintain oxygen partial pressure at a sufficiently high level to prevent excessive activation voltage loss at the cathode reaction layer. The average activation voltage losses, $\left|\eta^A\right|_{ave}$ and $\left|\eta^C\right|_{ave}$ can be calculated using Eqs. (21) and (57). The average reversible cell voltage, $E_{rev,ave}^{cell}$, should be calculated using Eq. (4) at the arithmetic average of the partial pressure values of hydrogen, oxygen, and water vapor at the anode and cathode channel inlets and exits. Then, the cell actual average voltage can be computed from the following equation:

$$V_{ave}^{cell} = E_{rev,ave}^{cell} - \eta_{\Omega,ave}^{t} - \left(\left|\eta^A\right|_{ave} + \left|\eta^C\right|_{ave}\right) - \eta^m \tag{58}$$

where

$$\left|\eta^m\right| = m \exp\left(n i_{geom}\right) \tag{59}$$

where m =2.11x10^{-5} V, n =8 cm^2_{geom} A^{-1} [44], i_{geom} in [A cm^2_{geom}].

4. Single cell electric power and thermal efficiency

The magnitude of the cell electric power, [W], is given by

$$\left|\dot{W}^{cell}_{electric}\right| = V^{cell}_{ave} I^{cell}_{t} \tag{60}$$

The single cell thermal efficiency is given by

$$\eta^{cell}_{thermal} = \frac{2FV^{cell}_{ave}}{\left(-\Delta H^{o}_{T}\right)} \tag{61}$$

where ΔH^{o}_{T} = standard-state enthalpy of reaction, Eq. (3), at the cell temperature, T, per g-mile of hydrogen oxidized to water vapor, [J mol^{-1}].

5. Extension of the single cell formulation for the performance prediction of a stack of identical cells connected in series (steady-state, isothermal operation)

It is here assumed that the anode-side flow channels of the individual PEMFCs connected in series are fed with the identical rates of fuel (hydrogen or a gas mixture, containing hydrogen, from a fuel reformer). The cathode-side flow channels of the individual PEMFCs are also fed with the identical rates of oxidant, air. The fuel and oxidant (air) flows are in the same (i.e. parallel) flow direction.

For n PEMFCs connected in series, the stack electric power output is given by

$$\left|\dot{W}^{stack}_{electric}\right| = nV^{cell}_{ave} I^{stack}_{t} \quad , \qquad [W] \tag{62}$$

The cell stack thermal efficiency is given by the following desired equation

$$\eta^{stack}_{thermal} = \frac{2FV^{cell}_{ave}}{\left(-\Delta H^{o}_{T}\right)} = \eta^{cell}_{thermal} \tag{63}$$

The mathematical expressions to compute molar flow rates of chemical species at the stack exit can be found in the report by Sandhu.[40]

6. Concluding remarks

Development of a mathematical model to simulate the performance of a PEMFC at an elevated temperature has been presented. The presented model is deemed sufficiently rigorous, yet not unwieldy for its application. Effect of the reactant species mass transport on the electrochemical kinetic reaction rates in the cell anode and cathode reaction layers have been properly accounted for to correctly predict the electrochemical reaction overvoltages or activation voltage losses in the cell thin reaction layers. The single cell developed model formulation has been linked to the stack model equations to predict the performance of a stack of a number of identical PEMFCs connected in series. Provided the sufficiently accurate values of the mass transport, charge transport, and electrochemical kinetic parameters are made available, the presented model formulation can be employed to numerically simulate the

performance of a single PEMFC as well as of a stack of a number of identical PEMFCs connected in series, utilizing an electrolyte such as sulfonated polyarylene ether, PBO/PBI doped with phosphoric acid, or Nafion-Teflon-$Zr(HPO_4)_2$, at an elevated temperature ($\geq$ 100 $^{\circ}$C) for the isothermal and steady-state operating conditions.

References

1. Baschuk JJ, Li X. Modelling of polymer electrolyte membrane fuel cells with variable degrees of water flooding. *J Power Sources.* 2000;86:181-196.
2. Bernardi DM. Water balance calculations for solid polymer electrolyte fuel cells. *J Electrochem Soc.* 1990;137(11):3344-3350.
3. Bernardi DM, Verbrugge MW. A mathematical model of the solid polymer electrolyte fuel cell. *J Electrochem Soc.* 1992;139(9):2477-2491.
4. Berning T, Djilali N. Three dimensional computational analysis of transport phenomena in a PEM fuel cell. Paper presented at: Seventh Grove Fuel Cell Symposium, 2001; London.
5. Berning T, Djilali N. Three dimensional numerical analysis of fluid flow, heat and mass transfer. *J Power Sources.* 2002;106:284-294.
6. Berning T, Djilali N. Three dimensional computational analysis of transport phenomena in a PEM fuel cell - a parametric study. *J Power Sources.* 2003;124(2):440-452.
7. Bussel HPLHv, Koene FGH, Mallant RKAM. Dynamic model of solid polymer fuel cell water management. *J Power Sources.* 1998;71:218-222.
8. Costamagna P. Transport phenomena in polymeric membrane fuel cells. *Chem Eng Sci.* 2001;56:323-332.
9. Dannenberg K, Ekdunge P, Lindbergh G. Mathematical model of the PEMFC. *J Appl Electrochem.* 2000;30:1377-1387.
10. Dutta S, Shimpalee S, Zee JWV. Three dimensional numerical simulation of straight channel PEM fuel cells. *J Appl Electrochem.* 1999;29:135-146.
11. Dutta S, Shimpalee S, Zee JWV. Numerical prediction of mass exchange between cathode and anode channels in a PEM fuel cell. *Int J Heat and Mass Transfer.* 2029-2042 2001;44:2001.
12. Eikerling M, Kharkats YI, Kornyshev AA, et al. Phenomenological theory of electro-osmotic effect and water management in polymer electrolyte proton-conducting membranes. *J Electrochem Soc.* 1998;145(8):2684-2699.
13. Gurau V, Liu H, Kakac S. Two-dimensional model for proton exchange membrane fuel cells. *AIChE J.* 1998;44(11):2410-2422.
14. Hsing IM, Futerko P. Two-dimensional simulation of water transport in polymer electrolyte fuel cells. *Chem Eng Sci.* 2000;55:4209-4218.
15. Janssen GJM, Overvelde MLJ. Water transport in the proton-exchange-membrane fuel cell: measurements of the effective drag coefficient. *J Power Sources.* 2001;101:117-125.
16. Jen TC, Yan T, Chan SH. Chemical reacting transport phenomena in a PEM fuel cell. *Int J Heat and Mass Transfer.* 2003;46(22):4157-4168.
17. Lum KW, McGuirk JJ. Three-dimensional model of a complete polymer electrolyte membrane fuel cell - model formulation, validation and parametric studies. *J Power Sources.* 2005;143:103-124.

18. Maggio G, Recupero V, Pino L. Modeling polymer electrolyte fuel cells: an innovative approach. *J Power Sources.* 2001;101:275-286.
19. Neshat HN, Shimpalee S, Dutta S, et al. Predicting the effect of gas flow channel spacing on current density in PEM fuel cells. *Proc ASME Adv Energy Systems Division.* 1999;39:337-350.
20. Nguyen PT, Berning T, Djilali N. Computational model of a PEM fuel cell with serpentine gas flow channels. *J Power Sources.* 2004;130(1-2):149-157.
21. Nguyen TV, White RE. Water and heat management model for proton-exchange-membrane fuel cells. *J Electrochem Soc.* 1993;140(8):2178-2186.
22. Rowe A, Li X. Mathematical modeling of proton exchange membrane fuel cells. *J Power Sources.* 2001;102:82-96.
23. Scott K, Kraemer S, Sundmacher K. Gas and liquid mass transport in solid polymer electrolyte fuel cells. *Inst Chem Eng Symp Ser.* 1999(145):11-20.
24. Senn SM, Poulikakos D. Three dimensional computational modeling of polymer electrolyte fuel cells. Paper presented at: Proceedings Fuel Cell Research Symposium - Modeling and Experimental Validation, 2004.
25. Shimpalee S, Dutta S, Lee WK, et al. Effect of humidity on PEM fuel cell performance part II - numerical simulation. *Proc ASME Heat Transfer Div.* 1999;364-1:367-374.
26. Siegel NP, Ellis MW, Nelson DJ, et al. A two dimensional computational model of a PEMFC with liquid water transport. *J Power Sources.* 2004;128(2):173-184.
27. Singh D, Lu DM, Djilaki N. A two dimensional analysis of mass transport in proton exchange membrane fuel cells. *Int J Eng Sci.* 1999;37:431-452.
28. Springer TE, Zawodzinski TA, Gottesfeld S. Polymer electrolyte fuel cell model. *J Electrochem Soc.* 1991;138(8):2334-2342.
29. Squadrito G, Maggio G, Passalacqua E, et al. An empirical equation for polymer electrolyte fuel cell (PEFC) behaviour. *Journal of Applied Electrochemistry.* 1999;29(12):1449-1455.
30. Um S, Wang CY. Three dimensional analysis of transport and electrochemical reactions in polymer electrolyte fuel cells. *J Power Sources.* 2004;125(1):40-51.
31. Um S, Wang CY, Chen KS. Computational fluid dynamics modeling of proton exchange membrane fuel cells. *J Electrochem Soc.* 2000;147(12):4485-4493.
32. Weber AZ, Newman J. Transport in polymer-electrolyte membranes. I. Physical model. *J Electrochem Soc.* 2003 2003;150(7):A1008-A1015.
33. Weber AZ, Newman J. Transport in polymer-electrolyte membranes. II. Mathematical model. *J Electrochem Soc.* 2004;151(2):A311-A325.
34. Weber AZ, Newman J. Transport in polymer-electrolyte membranes. III. Model validation in a simple fuel-cell model. *J Electrochem Soc.* 2004;151(2):A326-A339.
35. Wohr M, Bolwin K, Schnurnberger W, et al. Dynamic modelling and simulation of a polymer membrane fuel cell including mass transport limitation. *Int J Hydrogen Energy.* 1998;23(3):213-218.
36. Yi JS, Nguyen TV. An along the channel model for proton exchange fuel cells. *J Electrochem Soc.* 1998;145(4):1149-1159.
37. Yi JS, Nguyen TV. Multicomponent transport in porous electrodes of proton exchange membrane fuel cells using the interdigitated gas distributors. *J Electrochem Soc.* 1999;146(1):38-45.
38. Zhou T, Liu H. A general three-dimensional model for proton exchange membrane fuel cells. *Int J Transport Phenomena.* 2001;3:177-198.

39. Sandhu SS, Saif YA, Fellner JP. A reformer performance model for fuel cell applications. *J Power Sources.* 2005;140:88-102.
40. Sandhu SS. *Fuel cell development for AEF and PAD applications.* University of Dayton; July 2004 2004. UDR-TR-2004-00068. 7-1 through 7-68.
41. McCabe WL, Smith JC, Harriott P. *Unit Operations of Chemical Engineering*. 5th ed. New York: McGraw-Hill; 1993.
42. Si Y, Kunz HR, Fenton JM. Nafion-Teflon-$Zr(HPO_4)_2$ composite membranes for high-temperature PEMFCs. *J Electrochem Soc.* 2004;151(4):A623-A631.
43. Ma C, Zhang L, Mukerjee S, et al. An investigation of proton conduction in select PEM'S and reaction layer interfaces-designed for elevated temperature operation. *J Membrane Science.* 2003;219(1-2).
44. Larminie J. *Fuel Cell Systems Explained*. 2nd ed. Chichester, West Sussex: Wiley; 2003.